

# Phenotypic diversity of circulating tumour cells in patients with metastatic castration-resistant prostate cancer

Andrew S. McDaniel<sup>\*</sup>, Roberta Ferraldeschi<sup>†,‡</sup>, Rachel Krupa<sup>§</sup>, Mark Landers<sup>§</sup>, Ryon Graf<sup>§</sup>, Jessica Louw<sup>§</sup>, Adam Jendrisak<sup>§</sup>, Natalee Bales<sup>§</sup>, Dena Marrinucci<sup>§</sup>, Zafeiris Zafeiriou<sup>†,‡</sup>, Penelope Flohr<sup>†</sup>, Spyridon Sideris<sup>†,‡</sup>, Mateus Crespo<sup>†</sup>, Ines Figueiredo<sup>†</sup>, Joaquin Mateo<sup>†,‡</sup>, Johann S. de Bono<sup>†,‡</sup>, Ryan Dittamore<sup>§</sup>, Scott A. Tomlins<sup>\*,†,\*,\*\*</sup> and Gerhardt Attard<sup>†,‡</sup>

<sup>\*</sup>Department of Pathology, University of Michigan Medical School, Ann Arbor, MI, USA, <sup>†</sup>The Institute of Cancer Research, London, UK, <sup>‡</sup>Royal Marsden NHS Foundation Trust, London, UK, <sup>§</sup>Epic Sciences, San Diego, CA, <sup>†</sup>Department Urology, and <sup>\*\*</sup>Comprehensive Cancer Center, Michigan Center for Translational Pathology, University of Michigan Medical School, Ann Arbor, MI, USA

A.S.M., R.F., S.A.T. and G.A. contributed equally to the work.

## Objectives

To use a non-biased assay for circulating tumour cells (CTCs) in patients with prostate cancer (PCa) in order to identify non-traditional CTC phenotypes potentially excluded by conventional detection methods that are reliant on antigen- and/or size-based enrichment.

## Patients and Methods

A total of 41 patients with metastatic castration-resistant PCa (mCRPC) and 20 healthy volunteers were analysed on the Epic CTC platform, via high-throughput imaging of DAPI expression and CD45/cytokeratin (CK) immunofluorescence (IF) on all circulating nucleated cells plated on glass slides. To confirm the PCa origin of CTCs, IF was used for androgen receptor (AR) expression and fluorescence *in situ* hybridization was used for *PTEN* and *ERG* assessment.

## Results

Traditional CTCs (CD45<sup>+</sup>/CK<sup>+</sup>/morphologically distinct) were identified in all patients with mCRPC and we also

identified CTC clusters and non-traditional CTCs in patients with mCRPC, including CK<sup>−</sup> and apoptotic CTCs. Small CTCs ( $\leq$ white blood cell size) were identified in 98% of patients with mCRPC. Total, traditional and non-traditional CTCs were significantly increased in patients who were deceased vs alive after 18 months; however, only non-traditional CTCs were associated with overall survival. Traditional and total CTC counts according to the Epic platform in the mCRPC cohort were also significantly correlated with CTC counts according to the CellSearch system.

## Conclusions

Heterogeneous non-traditional CTC populations are frequent in mCRPC and may provide additional prognostic or predictive information.

## Keywords

circulating tumour cells, liquid biopsy, metastatic castration-resistant prostate cancer, ERG, PTEN

## Introduction

Dissemination of cancer cells from primary sites into circulation and seeding of metastases is the underlying cause of mortality for most non-haematopoietic malignancies. Detection and enumeration of circulating tumour cells (CTCs) is associated with decreased progression-free survival and overall survival for a variety of tumours, including prostate cancer (PCa) [1–3]. Based on these findings, CTC

enumeration could be a valuable tool for disease response and progression monitoring. Additionally, CTCs can also be characterized for predictive biomarkers. Given that CTCs circulate at very low concentrations ( $10^{-6}$ – $10^{-7}$ ) [4], detection in millilitres of blood requires extremely sensitive and specific methods. Numerous technologies have been developed to this end [5,6], with the majority requiring an enrichment step based on differences in various physical (size and/or density) or biological variables (surface marker

expression) to distinguish CTCs from surrounding haematopoietic cells. For example, the CellSearch<sup>®</sup> CTC System, the only US Food and Drug Administration-cleared method for CTC detection [7], requires cells to contain a 4',6-diamidino-2-phenylindole positive (DAPI)-intact nucleus, lack expression of the haematopoietic marker CD45, express epithelial cell adhesion molecule (EpCAM) and cytokeratin (CK), and have a diameter >4 µm [7]. Enrichment technologies, however, will potentially fail to capture non-traditional tumour cells lacking the selected characteristic.

Indeed, recent reports using non-EpCAM or size-based selection techniques have underscored this point, revealing PCa CTCs with non-traditional phenotypes, describing heterogeneity in size [8], epithelial marker expression [9], cell integrity [10] and proliferation rate [11]; both between and within individual patients. CTCs isolated from men with metastatic PCa have also shown evidence of epithelial to mesenchymal transition, via detection of epithelial to mesenchymal transition-related transcription factors, expression of N-cadherin and vimentin, and loss of CK and E-cadherin expression [9]. The degree and scope of this heterogeneity within PCa CTC populations is incompletely described, however, as most approaches are only able to assess heterogeneity in a single variable.

Numerous studies have identified a relationship between CTC counts and disease progression or overall survival in metastatic castrate-resistant PCa (mCRPC) [2,3]. These studies have been based on single-parametric enrichment technologies which probably miss non-traditional CTC phenotypes that may have prognostic or therapeutic significance. In the present study, we use a non-biased assay technique (the Epic CTC platform) that retains all nucleated cells and interrogates them in a multiparametric fashion, analysing size, shape, DAPI staining and immunofluorescence (IF) antigen characterization (typically CD45 and CK expression). Concurrently, we evaluated both traditional (CD45<sup>+</sup>, CK<sup>+</sup>, morphologically distinct) and candidate non-traditional CTCs for PCa-specific molecular aberrations, including androgen receptor (AR) expression by IF, and *PTEN* deletion and *ERG* rearrangement by fluorescence *in situ* hybridization (FISH) [12–15]. Through this approach, we show that patients with mCRPC harbour a variety of non-traditional CTC phenotypes.

## Patients and Methods

### Sample Collection and Handling

Whole-blood samples were obtained from 41 unique patients, required to have histologically or biochemically confirmed prostate adenocarcinoma and planned for initiation of a new treatment for progressive mCRPC in the presence of castrate levels of serum testosterone (<50 ng/dL [1.73 nmol/L]), consistent with Prostate Cancer Clinical Trials Working

Group 2 (PCWG2) guidelines. After collection at the Royal Marsden, Sutton, UK, samples were shipped to Epic Sciences (San Diego, CA, USA) at ambient temperature. Sample collection for this study was approved by the Royal Marsden (London, UK) Research Ethics Committee (REC 04/Q0801/6) and by the Royal Marsden Committee for Clinical Research. Additionally, 21 samples were obtained from 20 consenting healthy adults by the Institute of Cancer Research (London, UK) or Epic Sciences, and processed in the same manner as patient samples. All samples were collected with informed consent. Patient and healthy volunteer demographics are summarized in Table 1. The median (range) blood sample transit time for patient samples was 32 (28–78) h. Additional draws from select patients were evaluated as needed for FISH.

**Table 1** Demographic and clinical characteristics of patients and healthy volunteers at the time of study inclusion.

Patients with CRPC		<i>n</i> = 41
Age, years		
Median		70
Range		40–82
Serum PSA, ng/mL		
Median		90
Range		2–2532
Lactate dehydrogenase, U/L		
Median		170
Range		112–678
Albumin, g/L		
Median		35
Range		24–42
Haemoglobin, g/dL		
Median		12.2
Range		8.3–15.5
Sites of metastases, <i>n</i> (%)		
Bone		39 (95)
Nodal		28 (68)
Visceral		13 (32)
ECOG performance score		
0		6 (15)
1		33 (80)
2		2 (5)
Previous CRPC therapies, <i>n</i>		
Median		3
Range		1–5
Previous therapies, <i>n</i> (%)		
Bicalutamide		41 (100)
Docetaxel		26 (63)
Cabazitaxel		4 (10)
Abiraterone		14 (34)
Enzalutamide		3 (7)
Investigational agents		13 (32)
Healthy volunteers		<i>n</i> = 20
Age, years		
Median		33.5
Range		21–53
Sex		
Male		10
Female		10
CRPC, castration-resistant prostate cancer; ECOG, Eastern Cooperative Oncology Group.		

## Blood Sample Preparation and Storage

Upon sample receipt, red blood cells were lysed and nucleated cells dispensed onto glass microscope slides according to methods previously described [16–18]. Up to 12 slides were prepared from each blood sample at  $3 \times 10^6$  cells/slide. Slides were then stored at  $-80^\circ\text{C}$  (stable for >1 year, A. Johnson, unpublished data). The number of slides created from each individual sample was determined by the volume of blood received and the white blood cell (WBC) count.

## Circulating Tumour Cell Identification and Protein Characterization on the Epic Platform

For CTC analysis, two slides from each patient sample were thawed, then stained by IF to distinguish CTCs from WBCs, as described previously [16–18]. In addition to DAPI, CD45 and CK, an additional antibody targeting the N-terminal region of AR (clone D6F11; Cell Signalling Technology, Danvers, MA, USA) was used, capable of detecting full-length and LBD-truncated variants of the protein. Stained slides were imaged on a high-speed fluorescent imaging system. Captured images were analysed using an automated algorithm that characterizes each cell using >90 variables, including protein expression and morphology to distinguish CTCs from normal nucleated cells. All CTC candidates were then reviewed by trained technicians, and  $\text{CK}^+/\text{CD45}^-$  cells with intact,  $\text{DAPI}^+$  nuclei exhibiting tumour-associated morphologies were classified as traditional CTCs. The trained technicians were blinded as to whether the sample was from a patient with PCa or healthy donor. Candidate CTCs that did not meet the criteria for traditional CTC, as described in the Results section, were identified as  $\text{CD45}^-/\text{CK}^-$  cells with abnormal morphology or apoptotic CTCs ( $\text{CD45}^-$  with characteristic nuclear fragmentation or condensation). In a separate subsequent analysis, cell morphological characteristics, including cell area, were determined for each CTC using Epic proprietary software. Analysis was reviewed by a Board-certified Anatomical Pathologist with experience in genitourinary pathology and molecular characterization of mCRPC (S.A.T.) to confirm cancer origin.

## Circulating Tumour Cell Analysis via CellSearch Assay

Circulating tumour cell isolation and enumeration were carried out using the CellSearch™ system (Janssen Diagnostics, Raritan, NJ, USA) according to the manufacturer's instructions. Blood samples were drawn into CellSave™ tubes (Janssen Diagnostics) and samples were kept at room temperature and processed within 72 h of collection. To calculate the CTC count, 7.5 mL of blood was enriched immunomagnetically using anti-EpCAM antibodies, followed by fluorescent labelling and individual

capture using a four-colour semi-automated fluorescent microscope. The images were then presented to trained operators, who selected cells that met the definition of CTCs. The criteria used to define a CTC include round to oval morphology, size  $>5\ \mu\text{m}$ , a visible nucleus ( $\text{DAPI}^+$ ), positive staining for CK 8,18 and/or 19 (phycoerythrin) and negative staining for CD45 (allophycocyanin). Results were expressed as the number of cells per 7.5 mL of blood.

## Circulating Tumour Cell Fluorescence *in situ* Hybridization Analysis

After CTC IF analysis, a subset of slides with a sufficient number of CTCs was tested for *PTEN* loss or *ERG* rearrangements by FISH. Coverslips were removed and slides were hybridized using a two-color probe solution targeting either *PTEN* and chromosome 10 centromere (CC10) DNA sequences or regions flanking 5' and 3' *ERG* (Cymogen Dx, New Windsor, NY, USA). After processing, slides were counterstained with DAPI and mounted with an anti-fade mounting medium. Epic software was used to relocate CTCs for scoring. A minimum of 20 WBCs on each slide were also scored as internal controls.

*PTEN* loss was defined as a cell containing fewer *PTEN* signals than CC10 signals or only one of each signal (loss of chromosome 10). Cells with no *PTEN* signals and at least one CC10 signal were classified as homozygous *PTEN* loss. Heterozygous *PTEN* loss cells contained at least one *PTEN* signal and either more CC10 signals than *PTEN* or one *PTEN* signal and one CC10 signal. Cells with a 1:1 ratio of *PTEN*:CC10 and at least two of each signal were considered *PTEN* non-deleted. *ERG* rearrangements can present as a split of the 5' and 3' FISH signals (representing *ERG* fusions through insertion, inversion or translocation) or as a deletion of the 5' FISH signal (representing *TMPRSS2:ERG* fusions through deletion of the intervening region on chromosome 21). Hence, cells were considered *ERG*-rearranged if a separation of at least one pair of 5' and 3' *ERG* signals (by a distance of at least two signal diameters) or a deletion of at least one 5' *ERG* signal was observed. Cells in which all 3' *ERG* signals had a corresponding 5' *ERG* signal within two signal diameters were considered *ERG* non-rearranged.

## Statistical Analysis

Correlations/associations of traditional and non-traditional CTC counts and clinicopathological variables were assessed by Spearman rank correlation, two-sided Mann–Whitney tests, Kruskal–Wallis tests or Kaplan–Meier analysis using MEDCALC v 15.6 (MedCalc Software bvba, Belgium). Area under the curve from receiver–operator characteristic (ROC) curves was determined using MEDCALC v 15.6 for traditional and non-traditional CTC counts for predicting

mCRPC vs healthy volunteer status. Youden index CTC/mL threshold, value and CTC thresholds with sensitivity and specificity at 100% specificity and sensitivity, respectively, were determined as part of the ROC analysis. Kaplan–Meier analysis was performed by stratifying patients per CTC type into those with  $\leq$  vs  $>$  median CTC count. For all tests,  $P$  values  $<0.05$  were considered significant.

## Results

### Detection of Traditional Circulating Tumour Cells in Patients with Metastatic Castration-Resistant Prostate Cancer

A total of 41 blood samples from 41 patients with mCRPC and 21 blood samples from 20 healthy volunteers were analysed. Patient and healthy volunteer demographics are shown in Table 1. An average of 11 slides per patient were plated (range 4–16) from a mean (range) blood volume of 7.0 (3.68–7.83) mL per patient. Traditional CTCs were defined (described previously [16–18]) as cells with an intact, DAPI-positive nucleus lacking features of apoptosis, absence of CD45 staining (CD45<sup>−</sup>) and positive CK staining (CK<sup>+</sup>; Fig. 1). Additionally, traditional CTCs were required to have characteristic cytomorphological features consistent with malignancy (including nucleomegaly, nuclear membrane irregularity, eccentric cytoplasmic distribution, and polygonal/elongated cell shapes) [16–19]. Using this traditional CTC definition, 41/41 (100%) patients with mCRPC had detectable traditional CTCs (median [range] 5 [1–121]/mL) and 22/41 (54%) had  $>4$ /mL. When two or more adjacent traditional CTCs were identified, they were classified as CTC clusters. CTC clusters were detected in 7/41 (17%) patients (median [range] 0 [0–6]/mL; Fig. 1).

Of 20 healthy volunteers tested, none had  $>4$  events in 1 mL meeting the definition for a traditional CTC and 5(25%) had 1–4/mL (median [range] 0 [0–4]/mL; Fig. 2 for representative events in healthy volunteers). CTC clusters were not detected in healthy volunteer samples. Figure 3 shows the frequency of traditional CTCs and CTC clusters in patient samples compared with healthy volunteer samples.

An ROC curve analysis of traditional CTC counts, CTC clusters and other non-traditional CTCs as described below was performed to discriminate healthy volunteers from patients with mCRPC, although this is not the intended use of the assay (Table 2).

### Phenotypic and Molecular Characterization of Traditional Circulating Tumour Cells

Overexpression of AR, loss of *PTEN*, and *ERG* rearrangements (most commonly resulting in *TMPRSS2:ERG* gene fusions) are common molecular events in mCRPC and can be used to

confirm that captured cells are CTCs, especially *ERG* rearrangements that are PCa-specific [12–15]. AR expression was evaluated in all patients with mCRPC and select healthy volunteers. To generate a relative AR expression value for each CTC, Epic's software normalized AR expression in CTCs to approximately 1 million surrounding CD45<sup>+</sup> WBCs present on the same slide, resulting in CTCs with AR expression values  $\geq 3.0$  being considered positive. Across the 41 patients with mCRPC, 28 (68%) had at least one AR-positive traditional CTC/mL (range 0–96; Fig. 4A). The proportion of AR<sup>+</sup> to AR<sup>−</sup> traditional CTCs was variable (Fig. 4B). Of six healthy volunteer samples tested, none had  $>1$  AR<sup>+</sup> CTC/mL.

To further establish the prostatic origin of CTCs in our cohort, we also assessed *PTEN* and *ERG* status by FISH. First to determine assay specificity, we assessed *PTEN* and *ERG* status of WBCs from patient slides tested by FISH. Of 120 patient WBCs evaluated for *PTEN* FISH, 3 (2.5%) and 0 (0.0%) cells were detected with *PTEN* heterozygous and homozygous loss, respectively, resulting in 97.5–100% specificity of *PTEN* FISH on the Epic platform. Of 220 patient WBCs evaluated with *ERG* FISH, 10 (4.5%) and 0 (0.0%) cells had a split signal or loss of the 5' probe confirming 95.5–100% specificity.

After IF staining for CTC and AR detection on the Epic platform, CTCs from select patients with mCRPC were then relocated and evaluated for *PTEN* and/or *ERG* FISH status. *PTEN* deletions (heterozygous and/or homozygous) were detected in traditional CTCs from four of five patients evaluated (Table 3). Likewise, *ERG* rearrangements (translocation and/or deletion) were identified in traditional CTCs from five of six patients evaluated (Table 3). Representative images of traditional CTCs with AR expression and/or *PTEN* deletion or *ERG* rearrangement are shown in Fig. 1. Among slides from healthy volunteers, none had sufficient detectable CTCs to perform *PTEN* or *ERG* assessment.

### Detection of Non-Traditional Circulating Tumour Cells in Patients with Metastatic Castration-Resistant Prostate Cancer

As described in detail below, we identified two categories of cells with non-traditional phenotypes (in addition to CTC clusters) that were potential CTCs: cells with weak or no CK expression (CK<sup>−</sup> CTCs), and cells with degenerative changes and nuclear disintegration consistent with apoptosis (apoptotic CTCs). All patients harboured circulating cells with these non-traditional phenotypes (median 6/mL, range 1–101/mL). Four of 20 (20%) healthy volunteers had circulating cells that met these expanded CTC criteria (median 0/mL, range 0–5/mL) and 3/20 (15%) had cells with AR positivity (median 0/mL per patient, range 0–4/mL).



**Fig. 1** Patients with metastatic castration-resistant prostate cancer (mCRPC) harbour traditional and non-traditional circulating tumour cells (CTCs) with prostate cancer-specific molecular alterations. **(A)** Representative immunofluorescence (IF) image (100× magnification) examples of traditional and non-traditional CTCs in mCRPC patient samples (positive androgen receptor [AR] staining by IF is shown for each CTC). Traditional (DAPI<sup>+</sup>/CD45<sup>+</sup>/cytokeratin [CK]<sup>+</sup>/abnormal morphology), cluster (two or more adjacent traditional CTCs), small (DAPI<sup>+</sup>/CD45<sup>+</sup>/CK<sup>+</sup>/small cellular area), CK<sup>-</sup> (DAPI<sup>+</sup>/CD45<sup>+</sup>/CK<sup>-</sup>/AR<sup>+</sup>/abnormal morphology), and apoptotic (DAPI<sup>+</sup>/CD45<sup>+</sup>/CK<sup>-</sup>/nuclear disintegration/abnormal morphology) CTCs from mCRPC patient samples are shown. **(B)** Example photomicrographs (400× magnification) of *ERG* and *PTEN* gene alterations detected by fluorescence *in situ* hybridization (FISH) in traditional and non-traditional CTCs from mCRPC patient samples are shown (inset images (100× magnification) show CTC prior to FISH). *PTEN* deletions are indicated by loss of the *PTEN* locus green signal in the presence of chromosome 10 centromeric signal (CEP 10, red). *ERG* rearrangements can be identified by 5' deletion (resulting in loss of 5' green signal; far left panel) or by split 5'/3' signals (centre and second from right panel).

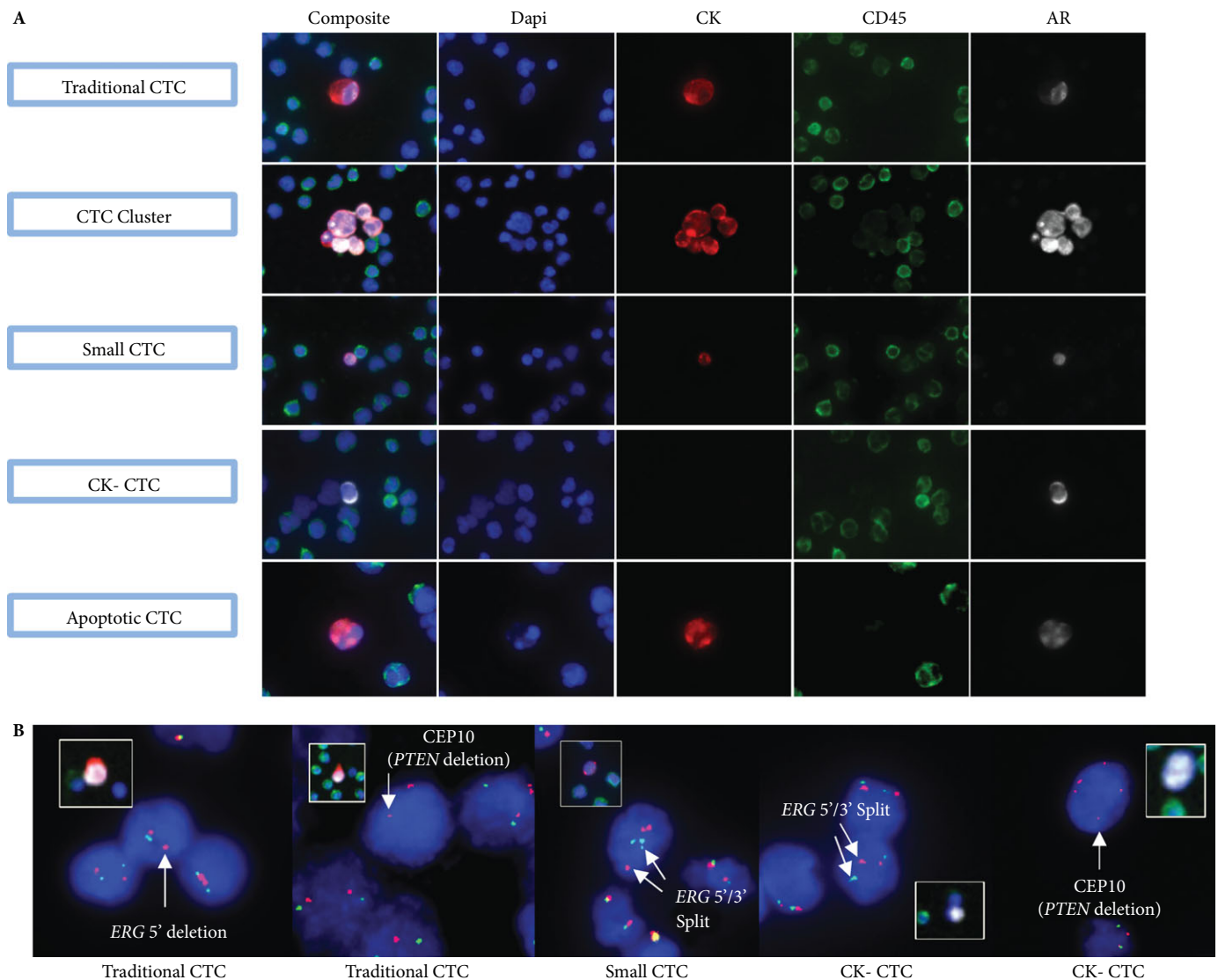
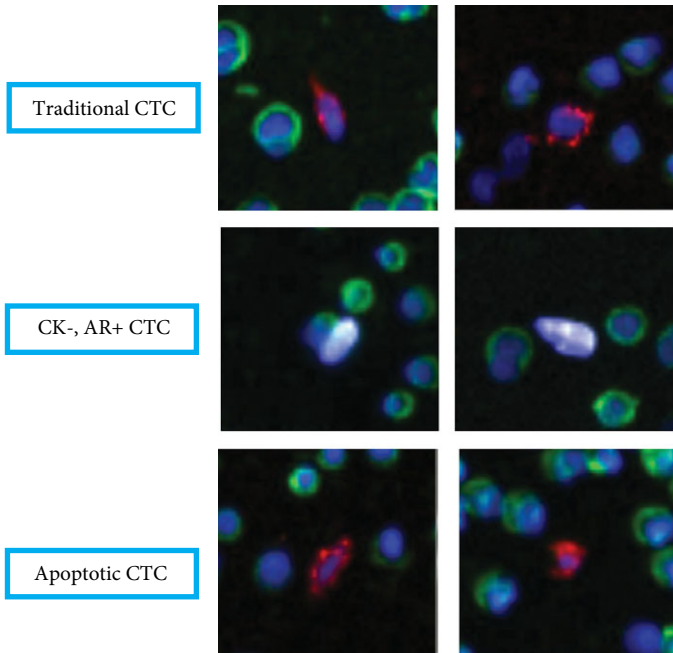


Figure 3 shows the frequency of non-traditional CTCs in patient samples compared with healthy volunteer samples. For all non-traditional CTCs, AR expression was evaluated by IF and showed a wide variability similar to traditional CTCs (Figure 4A). Representative images of non-traditional CTCs, including those with PCa-specific molecular alterations, are shown in Fig. 1.

### Cytokeratin-Negative Circulating Tumour Cells

Cytokeratin intensity in CD45<sup>+</sup> circulating cells with abnormal morphology varied widely across patients with mCRPC (Fig. 4C). As with AR expression measurements, relative CK expression values for every CTC were generated by Epic's software, normalizing CK expression in CTCs to

**Fig. 2** Circulating tumour cell (CTC)-like cells detected in healthy volunteers. Representative immunofluorescence (IF) examples (100× magnification) of traditional and non-traditional CTC-like cells in healthy volunteer samples. Traditional (DAPI<sup>+</sup>/CD45<sup>-</sup>/cytokeratin [CK]<sup>+</sup>/abnormal morphology), CK<sup>-</sup> (DAPI<sup>+</sup>/CD45<sup>-</sup>/CK<sup>-</sup>/androgen receptor (AR)<sup>+</sup>/abnormal morphology), and apoptotic (DAPI<sup>+</sup>/CD45<sup>-</sup>/CK<sup>+</sup>/nuclear disintegration/abnormal morphology) CTC-like cells from healthy volunteers are shown. Blue = DAPI, green = CD45, Red = CK, White = AR.



approximately 1 million surrounding CD45<sup>+</sup> WBCs present on the same slide. CTCs with CK expression values  $\geq 2.8$  were considered positive (signal  $\geq 2.8$ -fold higher than background WBCs). Hence, we defined non-traditional CK<sup>-</sup> CTCs as CD45<sup>-</sup> circulating cells with morphological distinction and/or

AR positivity, but CK intensity  $< 2.8$ . Such CK<sup>-</sup> CTCs were identified in 34/41 (83%) patients with mCRPC (median 2 CK<sup>-</sup> CTC/mL, range 0–20). Amongst patients with CK<sup>-</sup> CTCs, 26 (76%) had at least one AR<sup>+</sup> CK<sup>-</sup> CTC/mL (range 0–20). The proportion of CK<sup>+</sup>/CK<sup>-</sup> CTCs varied across the cohort, with two patients demonstrating a CTC population that was predominantly CK<sup>-</sup> (Fig. 4D). Of healthy volunteers evaluated, none had  $> 1$  CD45<sup>-</sup>/CK<sup>-</sup> cell/mL. *PTEN* FISH was performed on five representative patients with CK<sup>-</sup> CTCs and we were able to evaluate 18 CK<sup>-</sup> CTCs from three patients (Table 3). Of three patients with evaluable CK<sup>-</sup> CTCs, *PTEN* deletions were identified in one patient, with 5/9 (56%) CK<sup>-</sup> CTCs showing *PTEN* deletion. *PTEN* deletions were also detected in 4/11 (36%) traditional CTCs from this patient. *ERG* FISH was performed on six representative patients with CK<sup>-</sup> CTCs and we were able to evaluate 26 CK<sup>-</sup> CTCs from five patients. Of five patients with evaluable CK<sup>-</sup> CTCs, *ERG* rearrangements were identified in three patients, with 3/26 (12%) CK<sup>-</sup> CTCs showing *ERG* rearrangement. *ERG* rearrangements were also detected in 18/108 (17%) traditional CTCs from these three patients.

Apoptotic and Small Circulating Tumour Cells

CD45<sup>-</sup>/CK<sup>+</sup> cells with nuclear fragmentation or condensation characteristic of apoptosis were also observed across the mCRPC cohort. These cells, which we classified as non-traditional apoptotic CTCs, were detected in 40/41 (98%) of patients with mCRPC (median 4/mL, range 0–92/mL) as shown in Fig. 3. Of the 40 patients with apoptotic CTCs, 31 (78%) had at least one AR<sup>+</sup> apoptotic CTC/mL (range 0–60/mL). Similar to the other categories of non-traditional CTCs, the frequency of apoptotic CTCs varied among patients with mCRPC, with 11/41 (27%) patients

**Fig. 3** Circulating tumour cell (CTC) incidence in patients with metastatic castration-resistant prostate cancer (mCRPC) compared with healthy volunteers. **(A)** The number of traditional CTCs, CTC clusters, cytokeratin (CK)<sup>-</sup> CTCs, apoptotic CTCs and all CTC candidates (traditional, clusters, CK<sup>-</sup>, and apoptotic CTCs)/mL identified in healthy volunteers and mCRPC patient samples are plotted. Black lines indicate the median CTCs/mL. **(B)** Range, median, and mean CTCs/mL in mCRPC patient samples for all categories are given.

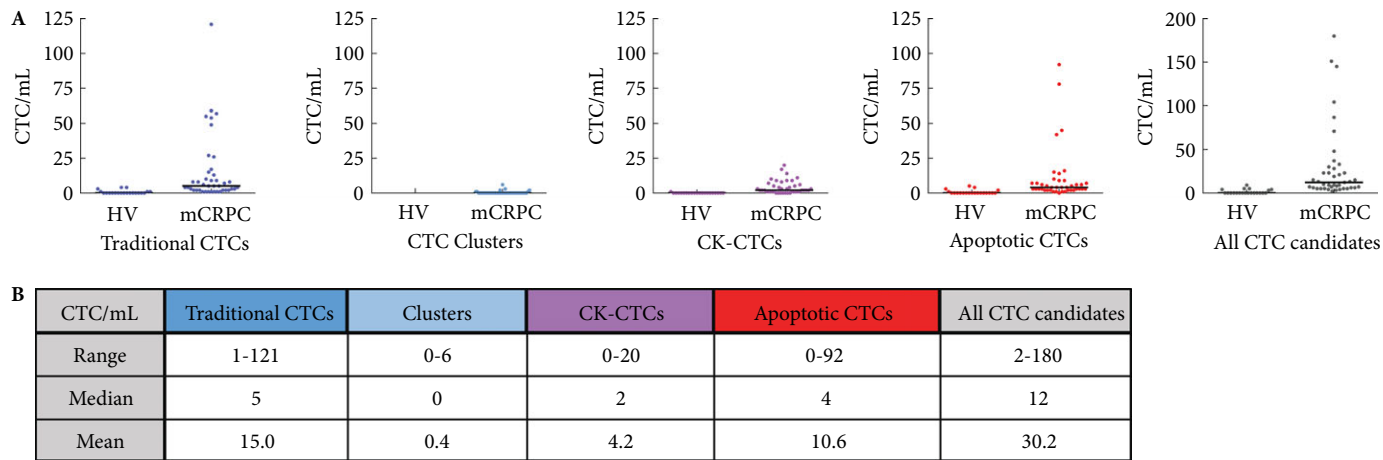


**Table 2** Receiver–operator characteristic curve analysis of circulating tumour cell counts for discriminating healthy volunteers and patients with metastatic castration-resistant prostate cancer.

CTC type	ROC		Youden index		100% sensitivity		100% specificity	
	Area under the curve	95% CI	Value	CTC/mL threshold	CTC/mL threshold	Specificity	CTC/mL threshold	Sensitivity
All CTCs	0.96	(0.88–0.99)	0.76	>4	>0	71%	>9	56%
Traditional CTCs	0.93	(0.84–0.98)	0.71	>0	>0	71%	>4	54%
Apoptotic CTCs	0.91	(0.81–0.97)	0.74	>0	N/A	N/A	>5	39%
CK <sup>−</sup> CTCs	0.91	(0.81–0.97)	0.78	>0	N/A	N/A	>1	63%
CTC clusters	0.59	(0.45–0.71)	0.17	>0	N/A	N/A	>0	17%

CK, cytokeratin; CRPC, castration-resistant prostate cancer; CTC, circulating tumour cell; ROC, receiver–operator characteristic. ROC curves were generated from CTC/mL counts for indicated CTC types (all CTCs is the sum of the other four types) for predicting CRPC status in 21 healthy volunteer samples (from 20 patients) and 41 CRPC samples. Cell size was not included in this analysis (all categories may include small nuclear-sized CTCs). Area under the curve and 95% CIs are given, along with Youden index values and CTC/mL thresholds. CTC/mL thresholds for 100% sensitivity and specificity are given, along with corresponding specificity and sensitivity.

exhibiting CTC populations composed primarily of apoptotic CTCs (Fig. 4E). As a result of nuclear fragmentation or disintegration, apoptotic CTCs were not amenable to FISH analysis.

We then used Epic software to objectively measure the total cell area of each CTC to elucidate the subpopulations of CTCs in patient samples that were similar in size to (or smaller than) WBCs, that could potentially be missed by size or density enrichment strategies for CTC isolation.

Approximately 300 patient WBCs were used to generate the median and interquartile ranges for WBC area (75  $\mu\text{m}^2$  and 64–90  $\mu\text{m}^2$ , respectively). We therefore used a cell area  $\leq 90 \mu\text{m}^2$  to define a small CTC (Fig. 5A). Using this approach, cell area of traditional and non-traditional CTC subtypes was evaluated for 40/41 patient samples (one sample was not evaluable by this method and was omitted from analysis). Apoptotic CTCs were omitted from analysis because of poor segmentation caused by fragmented cell morphology. We observed a wide range of CTC sizes within individual patients and across the cohort of patients with mCRPC using this objective assessment, with small CTCs detectable in 39/40 (97.5%) patients with mCRPC. CTCs detected in patients with mCRPC had a median (range) cell area of 99.0 (28.9–1631.0)  $\mu\text{m}^2$ . The proportion of small CTCs (CTCs with cell area  $\leq 90 \mu\text{m}^2$ ) is shown for each patient in Fig. 5B, with 17/40 (42.5%) patients exhibiting CTC populations composed predominantly of small CTCs. Small CTCs were evaluated in select patient samples by FISH for *ERG* and *PTEN* aberrations (Table 3). *ERG* FISH was performed on six patients with small CTCs and we were able to evaluate 27 small CTCs from three patients. Of these, *ERG* rearrangements were detected in one patient in 6/23 (26%) small CTCs. *ERG* rearrangements were also detected in 18/73 (25%) traditional CTCs (non-small) from this patient. The size of small CTCs precluded interpretation of *PTEN* deletions in all but three small CTCs in two patients, which were wild-type. Examples of small CTCs harbouring AR positivity by IF or *ERG* alterations by FISH are shown in Fig. 1. Examples of small CTCs harbouring

AR positivity by IF or *ERG* alterations by FISH are shown in Fig. 1.

### Clinical Significance of Circulating Tumour Cell Types

Although the main focus of the present study was to define the morphological and phenotypic range of CTCs in patients with mCRPC using an unbiased approach complemented by molecular characterization, we also assessed associations between traditional and non-traditional CTC types and clinicopathological variables (serum PSA, lactate dehydrogenase, albumin and haemoglobin levels, as well as previous treatment regimens and presence of visceral metastasis). Importantly, as shown in Fig. 6A, this analysis showed that counts of all CTC types detected by the Epic platform (traditional, CTC clusters and each non-traditional CTC type, as well as the sum of all CTCs) are significantly correlated with each other, ranging from Spearman rank correlation ( $r_s$ ) = 0.35 for apoptotic CTC and CTC cluster counts ( $P = 0.03$ ), to  $r_s = 0.72$  for traditional CTC and apoptotic CTC counts ( $P < 0.001$ ). Interestingly, there was no significant correlation between any CTC type count and serum PSA levels; however, counts of CTC types other than CTC clusters were significantly associated with high lactate dehydrogenase and low albumin, two important prognostic variables. Likewise, both all CTC (sum of traditional CTCs, CTC clusters, apoptotic CTCs and CK<sup>−</sup> CTCs) and apoptotic CTC counts were significantly associated with the presence of visceral metastasis (Fig. 6B). We did not identify a statistically significant difference between any CTC type count and previous treatment regimen.

Next, we assessed correlations between CTC counts according to the CellSearch CTC System and the Epic platform in the mCRPC cohort. Importantly, as shown in Table 4, we observed strong correlation between traditional CTC counts according to CellSearch and traditional CTCs

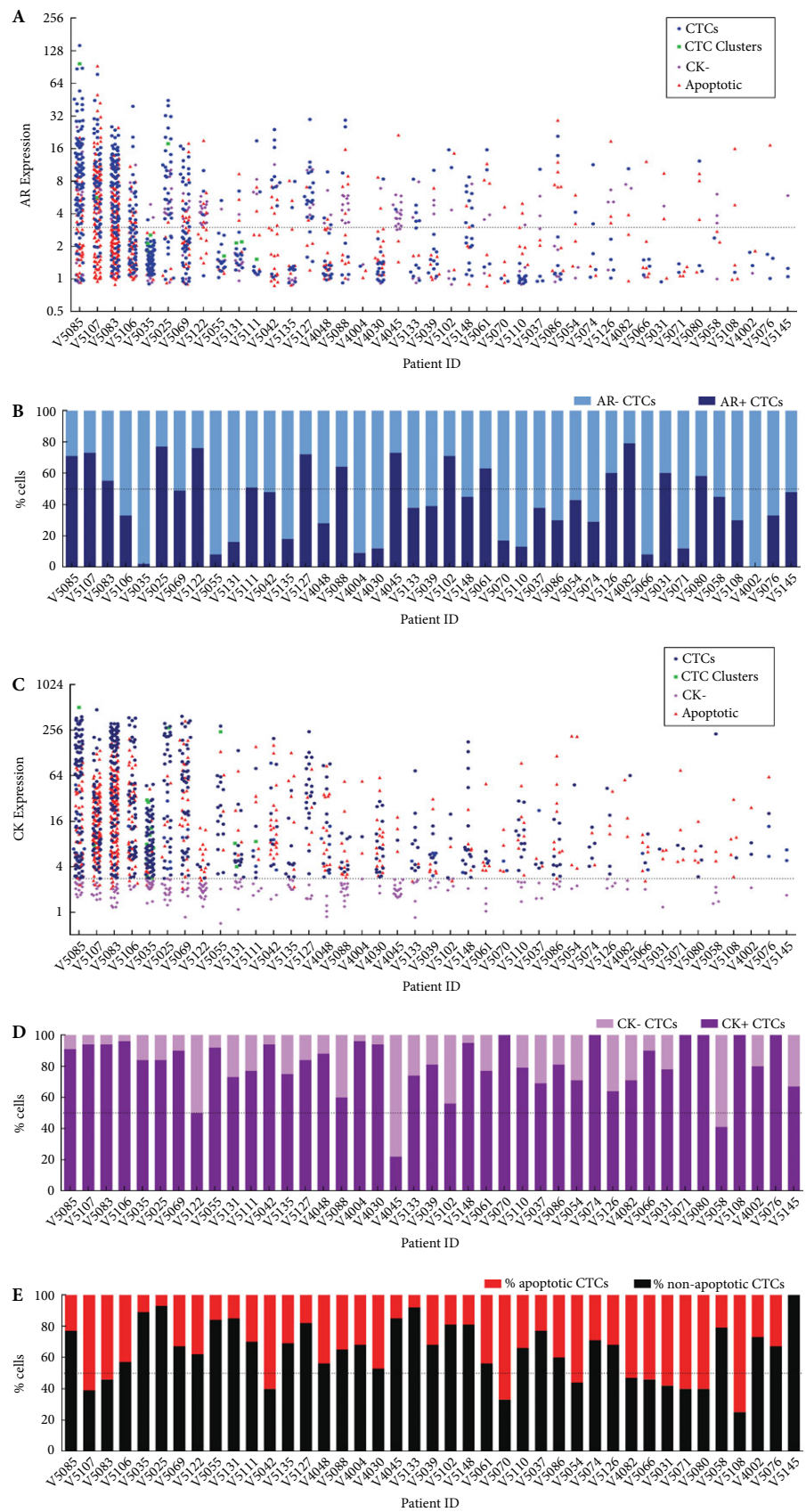




**Fig. 4** Androgen receptor (AR) and cytokeratin (CK) expression by immunofluorescence varies across traditional and non-traditional circulating tumour cell (CTCs) in metastatic castration-resistant prostate cancer (mCRPC) patient samples. AR (**A&B**) and CK (**C&D**) intensity distribution across traditional and non-traditional CTCs per patient. The dashed lines at 3 (**A**) and 2.8 units (**C**) indicate the threshold for AR and CK positivity, respectively. Charts B and D show the percentage of all CTCs/mL (traditional and non-traditional) with or without (**B**) AR or (**D**) CK expression per patient. (**E**) The percentage of apoptotic and non-apoptotic CTCs/mL per patient.

**Table 3** Fluorescence *in situ* hybridization characterization of prostate cancer (PCa)-specific molecular alterations (*PTEN* deletions top; *ERG* rearrangements bottom) in phenotypically diverse CTCs in patients with metastatic castration-resistant PCa.

Patient	Cell type	<i>PTEN</i> evaluable cells, <i>n</i>	AR <sup>+</sup> cells, %	<i>PTEN</i> heterozygous cells, <i>n</i>	<i>PTEN</i> homozygous cells, <i>n</i>	<i>PTEN</i> deletion cells <sup>†</sup> , %
V4004 <sup>†</sup>	Traditional	7	14	2	0	29
	CK <sup>-</sup>	0	N/A	N/A	N/A	N/A
	Small	0	N/A	N/A	N/A	N/A
V5035	Traditional	32	0	1	0	3%
	CK <sup>-</sup>	4	25	0	0	0
	Small	1	0	0	0	0
V5042 <sup>†</sup>	Traditional	11	36	0	4	37
	CK <sup>-</sup>	9	44	1	4	56
	Small	2	0	0	0	0
V5131	Traditional	12	0	1	1	17
	CK <sup>-</sup>	5	0	0	0	0
	Small	0	N/A	N/A	N/A	N/A
V5055	Traditional	13	0	0	0	0
	CK <sup>-</sup>	0	N/A	N/A	N/A	N/A
	Small	0	N/A	N/A	N/A	N/A
Patient	Cell type	<i>ERG</i> evaluable cells, <i>n</i>	AR <sup>+</sup> cells, %	<i>ERG</i> 5' deletion cells, <i>n</i>	<i>ERG</i> 5'/3' split cells, <i>n</i>	<i>ERG</i> rearranged cells <sup>†</sup> , %
V4048	Traditional	11	0 <sup>§</sup>	0	0	0
	CK <sup>-</sup>	0	N/A	N/A	N/A	N/A
	Small	0	N/A	N/A	N/A	N/A
V5025 <sup>†</sup>	Traditional	73	73	6	12	25
	CK <sup>-</sup>	10	90	0	0	0
	Small	23	48	2	4	26
V5083	Traditional	35	63	4	7	31
	CK <sup>-</sup>	2	100	0	1	50
	Small	3	0	0	0	0
V5085 <sup>†</sup>	Traditional	64	94	0	4	6
	CK <sup>-</sup>	6	83	0	1	17
	Small	0	N/A	N/A	N/A	N/A
V5106	Traditional	9	56	0	3	33
	CK <sup>-</sup>	1	100	0	1	100
	Small	0	N/A	N/A	N/A	N/A
V5131 <sup>†</sup>	Traditional	21	0	0	3	14
	CK <sup>-</sup>	7	0	0	0	N/A
	Small	1	100	0	0	N/A

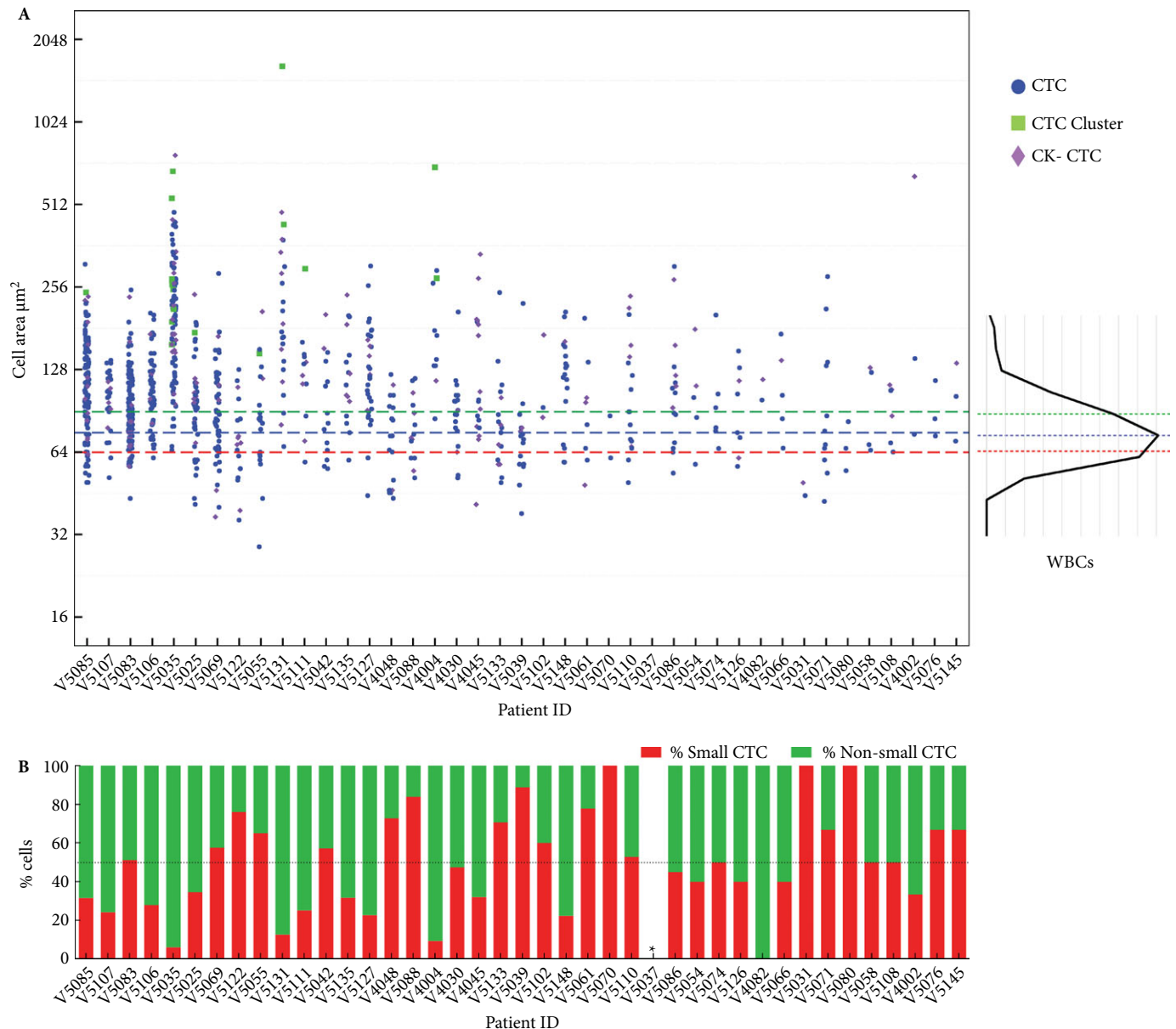
AR, androgen receptor; CK, cytokeratin. Fluorescence *in situ* hybridization (FISH) analysis for prostate-cancer specific alterations was performed on selected patients. The percentage of circulating tumour cells (CTCs; stratified by type) with AR positivity by immunofluorescence is given for patients assessed for *PTEN* loss (top panel) or *ERG* rearrangement (bottom) by FISH. False-positive *PTEN* heterozygous and homozygous rate in white blood cells (WBCs) 2.5% (3/120 WBCs) and 0% (0/120 WBCs), respectively. False-positive *ERG* 5' deletion and 5'/3' split rate 0% (0/220 WBCs) and 4.5% (10/220 WBCs), respectively. <sup>†</sup>Including both heterozygous and homozygous cells; <sup>‡</sup>Additional slides beyond the standard two slides were used for FISH evaluation; <sup>§</sup>Both 5' deletion and 5'/3' split cells; <sup>§</sup>Three cells were unevaluable for AR expression.

according to the Epic platform in the patients with mCRPC (Pearson's correlation  $r = 0.78$ ,  $P < 0.001$ ). Likewise, we also observed significant correlations between CellSearch CTC counts and apoptotic (Pearson's correlation  $r = 0.91$ ,  $P < 0.0001$ ) or CK<sup>-</sup> CTC counts ( $r = 0.39$ ,  $P = 0.02$ ) with the Epic platform (Table 4). No significant correlation was observed between CellSearch CTC counts and CTC cluster counts ( $r = -0.07$ ,  $P = 0.68$ ) according to the Epic platform, although CTC clusters were infrequently observed

in our cohort. Importantly, we identified a strong, significant correlation between CellSearch CTC counts and total CTC counts with the Epic platform ( $r = 0.89$ ,  $P < 0.001$ ; Table 4).

Lastly, to provide preliminary insight into associations with clinical outcome, we determined CTC counts with the Epic platform in patients with mCRPC who were alive and those who were dead after 18 months (40 of 41 patients with

**Fig. 5** Circulating tumour cell (CTC) size varies greatly across patients with metastatic castration-resistant prostate cancer (mCRPC). **(A)** Cellular area ( $\mu\text{m}^2$ ) per CTC as calculated by Epic software for each patient is plotted. White blood cell (WBC) size frequency distribution curve was generated by measuring the cellular area of approximately 300 normal WBCs (right side). The blue dashed line represents the median WBC area ( $75 \mu\text{m}^2$ ). Red and green dashed lines indicate WBC size cut-offs equal to the 25th ( $64 \mu\text{m}^2$ ) and 75th ( $90 \mu\text{m}^2$ ) percentile, respectively. Traditional CTCs (blue), CTC clusters (green) and CK<sup>+</sup> CTCs (purple) are indicated according to the legend. Apoptotic CTCs were omitted from analysis because of poor segmentation of fragmented nuclei in these cells. **(B)** The percentage of all CTCs for each patient with area greater than (non-small CTC; green) or less than the WBC 75th percentile (small CTC; red) is plotted. \*Sample 5037 was not evaluable and is not included in panel A.



sufficient follow-up). As shown in Fig. 6C, total, traditional and non-traditional (clusters, apoptotic and CK<sup>+</sup>) CTC counts were significantly higher in patients who had died compared with those who were alive at 18 months (Mann–Whitney test,  $P = 0.02$ ,  $P = 0.03$  and  $P = 0.04$ , respectively). On Kaplan–Meier analysis of all 41 patients, the number of non-traditional CTCs was significantly associated with

overall survival ( $>$  vs  $\leq$  median CTC count;  $P = 0.03$ ; Fig. 4D). Results for individual non-traditional CTC types are shown in Fig. 7. Interestingly, there were 14 patients with  $<5$  CTCs detected by the CellSearch assay, of which four were deceased at 18 months; each of these deceased patients had non-traditional CTC cells, as detected by the Epic platform.

**Fig. 6** Associations of circulating tumour cell (CTC)/mL counts and clinicopathological variables. **(A)** Spearman rank correlation ( $r_s$ ) matrix of CTC/mL counts (all = summed traditional, clusters, CK<sup>+</sup> and apoptotic) and clinicopathological variables for the 41 patients with metastatic castration-resistant prostate cancer (mCRPC) in our cohort. Correlations are given and indicated according to the colour scale in the legend. Statistical significance of each comparison is indicated by the cell border thickness according to the legend. **(B)** Significant ( $P < 0.05$ , Mann–Whitney test) associations between CTC counts (and clinicopathological variables) with the presence/absence of visceral metastases are shown. **(C)** All, traditional and non-traditional CTC counts stratified by patient status (dead vs alive) at 18 months are plotted (40 of 41 patients evaluable at that time point).  $P$  values from Mann–Whitney tests are shown. **(D)** Kaplan–Meier analysis for all, traditional and non-traditional CTC counts for overall survival time for all 41 patients. For each CTC type, patients were stratified by having  $>$  or  $\leq$  median CTC count/mL. Log-rank test  $P$  values are shown.

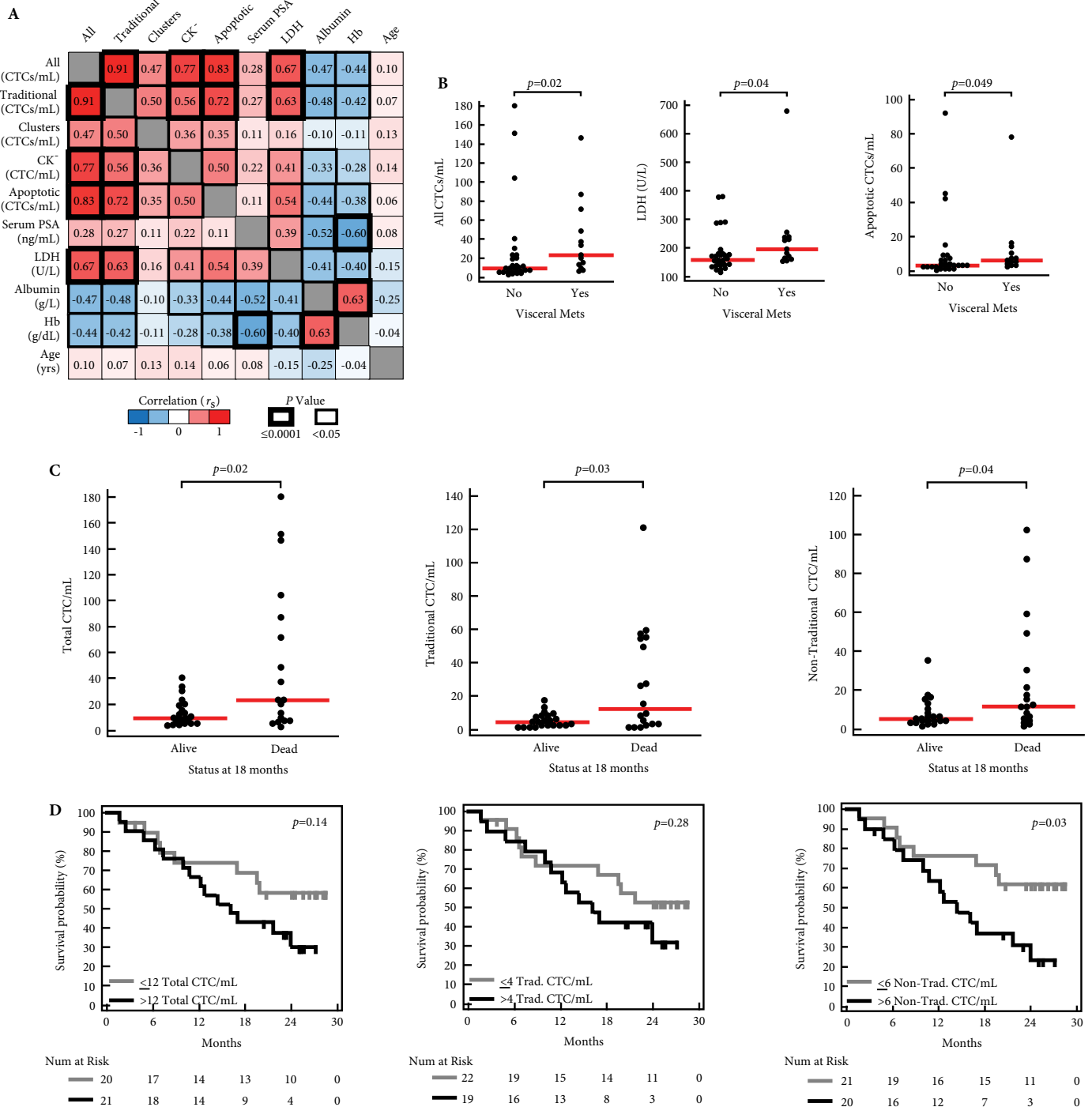


**Table 4** Circulating tumour cell counts according to the Epic vs CellSearch platforms in patients with metastatic castration-resistant prostate cancer.

Patient	CellSearch	Epic CTC counts				
	CTCs/7 mL	Traditional CTCs/mL	CTC Clusters /mL	CK <sup>+</sup> CTCs/mL	Apoptotic CTCs/mL	All CTCs/mL
V4002	NA	2	0	1	1	4
V4004	2	9	3	1	6	19
V4030	NA	7	0	1	7	15
V4045	NA	1	0	10	2	13
V4048	12	9	0	2	9	20
V4082	5	1	0	2	3	6
V5025	157	54	1	11	5	71
V5031	NA	1	0	1	3	5
V5035	1	57	6	14	10	87
V5037	0	4	0	3	2	9
V5039	27	6	0	2	4	12
V5042	285	8	0	1	14	23
V5054	11	1	0	2	4	7
V5055	52	26	2	3	6	37
V5058	1	1	0	3	1	5
V5061	6	3	0	2	4	9
V5066	NA	2	0	1	3	6
V5069	70	27	0	5	16	48
V5070	1	3	0	0	6	9
V5071	6	2	0	0	3	5
V5074	18	5	0	0	2	7
V5076	1	2	0	0	1	3
V5080	3	2	0	0	3	5
V5083	646	59	0	9	78	146
V5085	563	121	0	17	42	180
V5086	26	3	0	1	3	7
V5088	0	5	0	8	7	20
V5102	5	4	0	5	2	11
V5106	448	55	0	4	45	104
V5107	568	49	1	9	92	151
V5108	1	1	0	0	3	4
V5110	0	4	0	2	3	9
V5111	0	13	1	7	9	30
V5122	0	5	0	20	15	40
V5126	5	2	0	2	2	6
V5127	95	15	0	4	4	23
V5131	0	17	2	9	5	33
V5133	12	8	0	3	1	13
V5135	2	10	0	6	7	23
V5145	34	1	0	1	0	2
V5148	21	8	0	0	2	10
Correlation with CellSearch:		0.78	−0.07	0.39	0.91	0.89
<i>P</i>		<0.001	0.68	0.02	<0.001	<0.001

CK, cytokeratin; CTC, circulating tumour cell; NA, not available. CTC counts for 41 patients with metastatic castration-resistant prostate cancer as determined by the CellSearch and Epic platforms are given. For Epic determined CTC counts, counts for traditional CTCs, non-traditional CTCs (CTC clusters, apoptotic CTCs and CK<sup>+</sup> CTCs) and all CTCs (sum of traditional and non-traditional CTCs) are given. Pearson correlation and *P* values of CellSearch counts with each Epic CTC category across the cohort are given below the table.

## Discussion

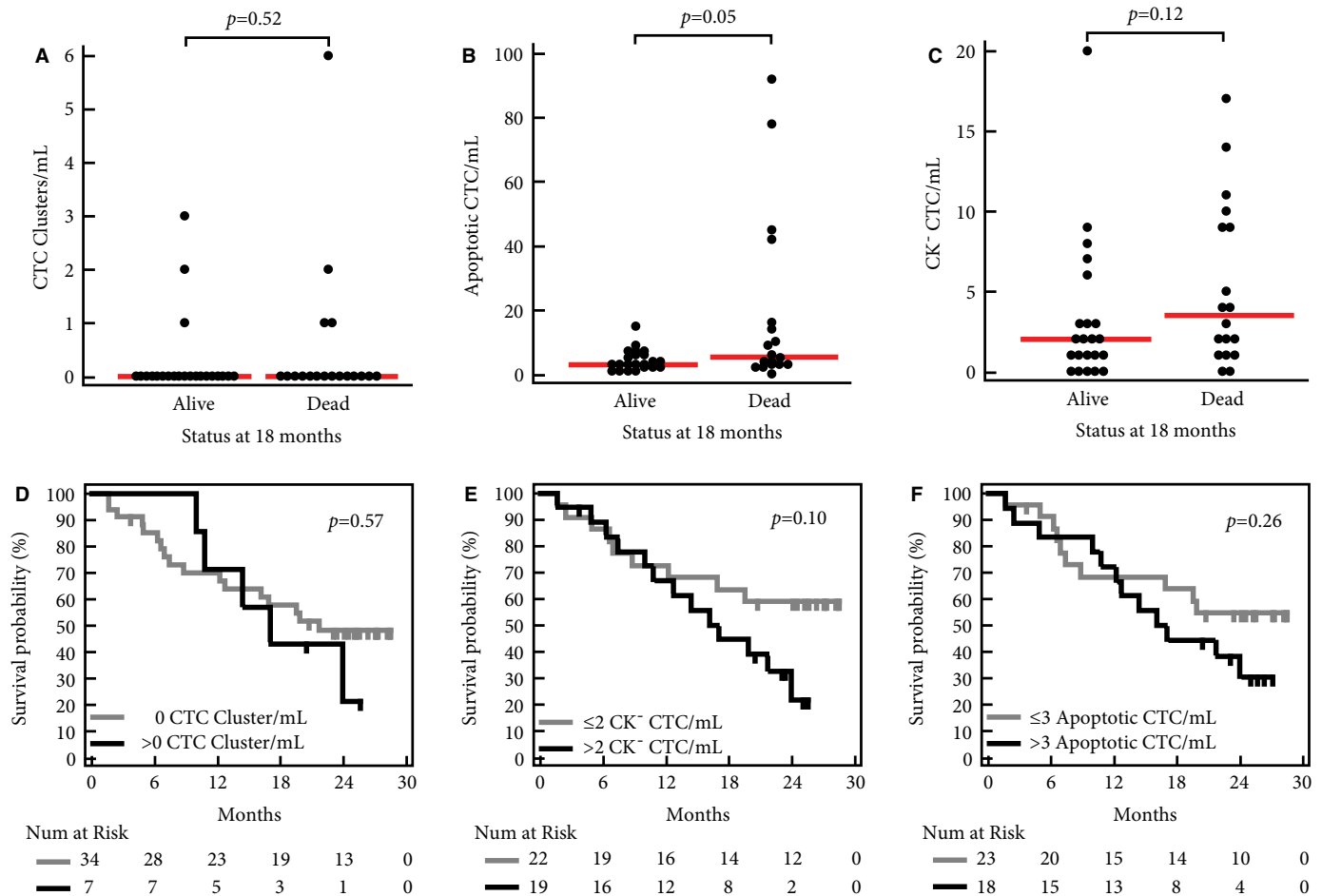
To characterize the phenotypic diversity of CTCs in mCRPC, we used the Epic platform to characterize all nucleated cells from whole-blood samples [20]. Using DAPI, CD45, CK and AR IF, we identified and morphologically characterized cells with cancer-associated features, irrespective of whether they met the traditional CTC definition. We then used FISH and slide scanning with single-cell resolution to confirm that subpopulations of non-traditional CTCs were PCa in origin. We detected non-traditional CTCs in all patients, including CTC clusters, small, apoptotic and/or CK<sup>+</sup> CTCs. We also observed intra-patient heterogeneity of AR and CK expression

and *PTEN* and *ERG* status consistent with a heterogeneous model of advanced disease, as has been observed in recent studies of CRPC assessing AR expression in CellSearch-isolated CTCs, metastatic tissues assessed by whole-genome sequencing, and circulating cell-free DNA assessed using targeted next-generation sequencing [21–23].

Although non-traditional CTC counts correlated with traditional CTC counts, substantial variation in the proportions of traditional to non-traditional CTCs were observed. Importantly, some CTCs we identified could be missed by CTC detection platforms using antigen capture (i.e. EpCAM or CK) or size selection (such as filtration). Similarly,



**Fig. 7** Associations of non-traditional circulating tumour cell (CTC)/mL counts in patients with metastatic castration-resistant prostate cancer and overall survival (**A–C**). Individual non-traditional CTC type counts (CTC clusters (**A**), apoptotic CTCs (**B**), and cytokeratin [CK]<sup>−</sup> CTCs (**C**) stratified by patient status (dead vs alive) at 18 months are plotted (40 of 41 patients evaluable at that time point). *P* values from Mann–Whitney tests are shown. (**D–F**) Kaplan–Meier analysis for CTC clusters (**D**), CK<sup>−</sup> CTCs (**E**), and apoptotic CTCs (**F**), and overall survival time for all 41 patients are shown. For each CTC type, patients were stratified by having > or ≤ median CTC count/mL. Log-rank test *P* values are shown.



Chen et al. [8], recently reported that EpCAM captured CTCs (enriched using NanoVelcro Chips) in patients with mCRPC showed variable nuclear size, and patients with visceral metastases specifically showed elevated very small nuclear-sized CTCs [8]. Our results suggest that in addition to nuclear size variability, CTCs in patients with mCRPC show considerable heterogeneity in nuclear organization, and CK and AR expression.

CK<sup>+</sup>/CD45<sup>−</sup> cells were identified in a small minority of healthy volunteer samples at low frequencies, with the majority demonstrating low CK and AR expression. Given no universally established reference range for the definition of CTCs, nor a recognized pan-CTC marker, it is difficult to discern the relevance of these cells in healthy volunteers. CTC-like cells can be detected in the blood of patients with benign conditions as well as in those with early-stage disease [24–26], and have been reported in labelled healthy

volunteers [27]. The ideal healthy volunteer or non-cancer control population would be matched in age and demographics, with confirmed absence of malignancy. While these caveats are impediments for using any CTC platform for the primary diagnosis of PCa, the increased sensitivity and specificity of the Epic platform for CTC detection could be suited for acquiring prognostic and predictive information in patients with mCRPC.

Detection of significant non-traditional CTC populations in patients with mCRPC is consistent with substantial evidence supporting their existence and clinical relevance. For example, CTCs postulated to have undergone epithelial to mesenchymal transition, and displaying reduced/no EpCAM or CK expression, have been identified by multiple platforms using both cell lines and patient samples [27–33]. These cells may be enriched for multipotent cancer stem cells, with increased self-renewal

and metastasis-forming capacity [34,35]. Although previous studies demonstrate substantial heterogeneity of *PTEN* deletion status in CTCs and CRPC tissue foci in a given patient [12,36], *ERG* rearrangements have generally been identified as a clonal alteration (when present) in both CTCs and mCRPC tissue [12,21,37–39]. Possible explanations for these apparently discrepant results include increased sensitivity for traditional and non-traditional CTCs (identified in the present study) that may represent multiple clonal populations when compared with our previous CellSearch-based study showing homogeneous *ERG* status in traditional CTCs [12]. Also, our recent study on circulating cell-free DNA in patients with mCRPC supported the existence of both *ERG* rearranged and wild-type clones in the same patient during disease progression [23]. This contrasts with the observation that multiple CRPC foci at autopsy in an individual patient nearly always show homogeneous *ERG* status. Further studies are required to interrogate this difference, which we hypothesize could be informed by more comprehensive genetic analysis of individual traditional and non-traditional CTC populations.

Our cohort represents a single-institution mCRPC cohort and the relatively small size in this non-uniformly treated initial study limits the ability to draw robust conclusions on associations between non-traditional CTCs and clinical outcome. Likewise, additional studies are needed to characterize the metastatic potential of distinct CTC classes. Importantly, evaluation of these distinct CTC populations described here in larger, well-defined cohorts to inform on their prognostic and predictive utility in mCRPC is now warranted. In the present study, using pathological and molecular biological approaches, we have described expanded categories of CTC phenotypes in patients with mCRPC and show that considerable heterogeneity exists within these categories. These expanded CTC subtypes may provide novel prognostic and predictive information for patients with mCRPC, as well as other advanced cancers. Intriguing preliminary clinical associations between mCRPC outcomes and various CTC subpopulations will need to be assessed in additional ongoing and planned studies to expand on our study.

## Acknowledgements

This work was in-part supported by funding from the Movember GAP CTC programme, National Institute for Health Research to The Royal Marsden/Institute of Cancer Research Biomedical Research Centre and National Institutes of Health (R01 CA183857 to S.A.T.). G.A. is a Cancer Research UK clinician scientist. We thank the participating men and their families who had metastatic PCa and nonetheless gave the gift of participation so that others might benefit.

## Conflict of Interest

The University of Michigan has been issued a patent on the detection of ETS gene fusions in PCa, on which Scott A. Tomlins is listed as a co-inventor. The University of Michigan licensed the diagnostic field of use to Gen-Probe, Inc., who has sublicensed some rights to Ventana/Roche. Scott A. Tomlins serves as a consultant to, and has received honoraria from, Ventana/Roche, Astellas, Medivation and Abbvie, and is a co-founder of Strata Oncology. Rachel Krupa, Mark Landers, Ryon Graf, Jessica Louw, Adam Jendrisak, Natalee Bales, Dena Marrinucci and Ryan Dittamore are employees of Epic Sciences. Roberta Ferraldeschi, Zafeiris Zafeiriou, Penelope Flohr, Spyridon Sideris, Joaquin Mateo, Johann S. de Bono and Gerhardt Attard are employees of The Institute of Cancer Research that has developed abiraterone and therefore has a commercial interest in this agent. Gerhardt Attard is on the ICR list of rewards to inventors for abiraterone. Johann S. de Bono has received consulting fees and travel support from Amgen, Astellas, AstraZeneca, Boehringer Ingelheim, Bristol-Myers Squibb, Dendreon, Enzon, Exelixis, Genentech, GlaxoSmithKline, Medivation, Merck, Novartis, Pfizer, Roche, Sanofi-Aventis, Supergen and Takeda, and grant support from AstraZeneca and Genentech. Gerhardt Attard has received honoraria, consulting fees or travel support from Astellas, Medivation, Janssen, Millennium Pharmaceuticals, Ipsen, Ventana and Sanofi-Aventis, and grant support from Janssen, AstraZeneca and Arno.

## References

- 1 Miyamoto DT, Sequist LV, Lee RJ. Circulating tumour cells-monitoring treatment response in prostate cancer. *Nat Rev Clin Oncol* 2014; 11: 401–12
- 2 Diamond E, Lee GY, Akhtar NH et al. Isolation and characterization of circulating tumor cells in prostate cancer. *Front Oncol* 2012; 2: 131
- 3 Armstrong AJ, Eisenberger MA, Halabi S et al. Biomarkers in the management and treatment of men with metastatic castration-resistant prostate cancer. *Eur Urol* 2012; 61: 549–59
- 4 de Cremoux P, Extra JM, Denis MG et al. Detection of MUC1-expressing mammary carcinoma cells in the peripheral blood of breast cancer patients by real-time polymerase chain reaction. *Clin Cancer Res* 2000; 6: 3117–22
- 5 Krebs MG, Metcalf RL, Carter L, Brady G, Blackhall FH, Dive C. Molecular analysis of circulating tumour cells-biology and biomarkers. *Nat Rev Clin Oncol* 2014; 11: 129–44
- 6 Hong B, Zu Y. Detecting circulating tumor cells: current challenges and new trends. *Theranostics* 2013; 3: 377–94
- 7 Cristofanilli M, Budd GT, Ellis MJ et al. Circulating tumor cells, disease progression, and survival in metastatic breast cancer. *N Engl J Med* 2004; 351: 781–91
- 8 Chen JF, Ho H, Lichterman J et al. Subclassification of prostate cancer circulating tumor cells by nuclear size reveals very small nuclear circulating tumor cells in patients with visceral metastases. *Cancer* 2015; 121: 3240–51

- 9 Armstrong AJ, Marengo MS, Oltean S et al. Circulating tumor cells from patients with advanced prostate and breast cancer display both epithelial and mesenchymal markers. *Mol Cancer Res* 2011; 9: 997–1007
- 10 Larson CJ, Moreno JG, Pienta KJ et al. Apoptosis of circulating tumor cells in prostate cancer patients. *Cytometry A* 2004; 62: 46–53
- 11 Stott SL, Lee RJ, Nagrath S et al. Isolation and characterization of circulating tumor cells from patients with localized and metastatic prostate cancer. *Sci Transl Med* 2010; 2: 25ra3.
- 12 Attard G, Swennenhuis JF, Olmos D et al. Characterization of ERG, AR and PTEN gene status in circulating tumor cells from patients with castration-resistant prostate cancer. *Cancer Res* 2009; 69: 2912–8
- 13 Beltran H, Rubin MA. New strategies in prostate cancer: translating genomics into the clinic. *Clin Cancer Res* 2013; 19: 517–23
- 14 Brenner JC, Chinnaiyan AM, Tomlins SA. ETS fusion genes in prostate cancer. In Tindall DJ ed, *Prostate Cancer: Biochemistry, Molecular Biology and Genetics*, Vol. Protein Reviews. New York: Springer New York, 2013: 139–83.
- 15 Grasso CS, Wu YM, Robinson DR et al. The mutational landscape of lethal castration-resistant prostate cancer. *Nature* 2012; 487: 239–43
- 16 Hsieh HB, Marrinucci D, Bethel K et al. High speed detection of circulating tumor cells. *Biosens Bioelectron* 2006; 21: 1893–9
- 17 Marrinucci D, Bethel K, Bruce RH et al. Case study of the morphologic variation of circulating tumor cells. *Hum Pathol* 2007; 38: 514–9
- 18 Marrinucci D, Bethel K, Kolatkar A et al. Fluid biopsy in patients with metastatic prostate, pancreatic and breast cancers. *Phys Biol* 2012; 9: 016003
- 19 Marrinucci D, Bethel K, Luttgen M, Bruce RH, Nieva J, Kuhn P. Circulating tumor cells from well-differentiated lung adenocarcinoma retain cytomorphologic features of primary tumor type. *Arch Pathol Lab Med* 2009; 133: 1468–71
- 20 Werner SL, Graf RP, Landers M et al. Analytical Validation and Capabilities of the Epic CTC Platform: enrichment-Free Circulating Tumour Cell Detection and Characterization. *J Circ Biomark* 2015; 4: 3
- 21 Gundem G, Van Loo P, Kremeyer B et al. The evolutionary history of lethal metastatic prostate cancer. *Nature* 2015; 520: 353–7
- 22 Crespo M, van Dalum G, Ferraldeschi R et al. Androgen receptor expression in circulating tumour cells from castration-resistant prostate cancer patients treated with novel endocrine agents. *Br J Cancer* 2015; 112 (Suppl): 1166–74
- 23 Carreira S, Romanel A, Goodall J et al. Tumor clone dynamics in lethal prostate cancer. *Sci Transl Med* 2014; 6: 254ra125
- 24 Miller MC, Doyle GV, Terstappen LW. Significance of circulating tumor cells detected by the cell search system in patients with metastatic breast colorectal and prostate cancer. *J Oncol* 2010; 2010: 617421
- 25 Pantel K, Deneve E, Nocca D et al. Circulating epithelial cells in patients with benign colon diseases. *Clin Chem* 2012; 58: 936–40
- 26 Reyat F, Valet F, de Cremoux P et al. Circulating tumor cell detection and transcriptomic profiles in early breast cancer patients. *Ann Oncol* 2011; 22: 1458–9
- 27 Ozkumur E, Shah AM, Ciciliano JC et al. Inertial focusing for tumor antigen-dependent and -independent sorting of rare circulating tumor cells. *Sci Transl Med* 2013; 5: 179ra47.
- 28 Pecot CV, Bischoff FZ, Mayer JA et al. A novel platform for detection of CK<sup>+</sup> and CK<sup>−</sup> CTCs. *Cancer Discov* 2011; 1: 580–6
- 29 Watanabe M, Uehara Y, Yamashita N et al. Multicolor detection of rare tumor cells in blood using a novel flow cytometry-based system. *Cytometry A* 2014; 85: 206–13
- 30 Giordano A, Gao H, Anfossi S et al. Epithelial-mesenchymal transition and stem cell markers in patients with HER2-positive metastatic breast cancer. *Mol Cancer Ther* 2012; 11: 2526–34
- 31 Yu M, Bardia A, Wittner BS et al. Circulating breast tumor cells exhibit dynamic changes in epithelial and mesenchymal composition. *Science* 2013; 339: 580–4.
- 32 Gorges TM, Tinhofer I, Drosch M et al. Circulating tumour cells escape from EpCAM-based detection due to epithelial-to-mesenchymal transition. *BMC Cancer* 2012; 12: 178
- 33 Zhang L, Ridgway LD, Wetzel MD et al. The identification and characterization of breast cancer CTCs competent for brain metastasis. *Sci Transl Med* 2013; 5: 180ra48.
- 34 Kalluri R, Weinberg RA. The basics of epithelial-mesenchymal transition. *J Clin Invest* 2009; 119: 1420–8
- 35 Scheel C, Weinberg RA. Cancer stem cells and epithelial-mesenchymal transition: concepts and molecular links. *Semin Cancer Biol* 2012; 22: 396–403
- 36 Ferraldeschi R, Nava Rodrigues D, Riisnaes R et al. PTEN Protein Loss and Clinical Outcome from Castration-resistant Prostate Cancer Treated with Abiraterone Acetate. *Eur Urol* 2015; 67: 795–802
- 37 Udager AM, Shi Y, Tomlins SA et al. Frequent discordance between ERG gene rearrangement and ERG protein expression in a rapid autopsy cohort of patients with lethal, metastatic, castration-resistant prostate cancer. *Prostate* 2014; 74: 1199–208
- 38 Mehra R, Tomlins SA, Yu J et al. Characterization of TMPRSS2-ETS gene aberrations in androgen-independent metastatic prostate cancer. *Cancer Res* 2008; 68: 3584–90
- 39 Liu W, Laitinen S, Khan S et al. Copy number analysis indicates monoclonal origin of lethal metastatic prostate cancer. *Nat Med* 2009; 15: 559–65

**Correspondence:** Scott A. Tomlins, University of Michigan Medical School, Institute of Cancer Research and the Ann Arbor, MI 48109-2200, USA. and Gerhardt Attard, The Institute of Cancer Research, London SM2 5NG, UK.

**e-mails:** tomlinss@umich.edu and gerhardt.attard@icr.ac.uk

**Abbreviations:** CTC, circulating tumour cell; PCa, prostate cancer; mCRPC, metastatic castration-resistant prostate cancer; EpCAM, epithelial cell adhesion molecule; CK, cytokeratin; FISH, fluorescence *in situ* hybridization; IF, immunofluorescence; AR, androgen receptor; WBC, white blood cell; CC10, chromosome 10 centromere; ROC, receiver–operator characteristic.